Original Paper

Cerebrovascular Diseases

Cerebrovasc Dis 2011;32:567–576
DOI: 10.1159/000331934

Received: February 7, 2011
Accepted: August 10, 2011
Published online: November 18, 2011

A New Image-Based Stroke Registry Containing Quantitative Magnetic Resonance Imaging Data

Dong-Eog Kim[a, b] Kyoung-Jong Park[c] Dawid Schellingerhout[g]
Sang-Wuk Jeong[a, b] Myung-Goo Ji[a] Won Jun Choi[b] Yoon-Oh Tak[d]
Geon-Hwan Kwan[c] Eun Ah Koh[f] Sang-Mi Noh[a] Hyung Yeol Jang[a]
Tae-Yun Kim[c] Ji-Won Jeong[f] Jae Sung Lee[e] Heung-Kook Choi[c]

[a]Department of Neurology, Dongguk University Ilsan Hospital, Dongguk University College of Medicine, and [b]Molecular Imaging and Neurovascular Research Laboratory, Dongguk University Ilsan Hospital, Goyang, Departments of [c]Computer Science and [d]Medical Imaging Science, Inje University, Gimhae, and [e]Department of Nuclear Medicine, Seoul National University Hospital, Seoul, Republic of Korea; [f]Department of Biochemistry and Cell Biology, William Marsh Rice University, and [g]Departments of Radiology and Experimental Diagnostic Imaging, University of Texas, MD Anderson Cancer Center, Houston, Tex., USA

Key Words
Alphanumeric data · Image-based stroke registry · Quantitative magnetic resonance imaging data

Abstract
Background: Conventional stroke registries contain alphanumeric text-based data on the clinical status of stroke patients, but this format captures imaging data in a very limited form. There is a need for a new type of stroke registry to capture both text- and image-based data. ***Methods and Results:*** We designed a next-generation stroke registry containing quantitative magnetic resonance imaging (MRI) data, 'DUIH_SRegI', developed a supporting software package, 'Image_QNA', and performed experiments to assess the feasibility and utility of the system. Image_QNA enabled the mapping of stroke-related lesions on MR onto a standard brain template and the storage of this extracted imaging data in a visual database. Interuser and intrauser variability of the lesion mapping procedure was low. We compared the results from the semi automatic lesion registration using Image_QNA with automatic lesion registration using SPM5 (Statistical Parametric Mapping version 5), a well-regarded standard neuroscience software package, in terms of lesion location, size and shape, and found Image_QNA to be superior. We assessed the clinical usefulness of an image-based registry by studying 47 consecutive patients with first-ever lacunar infarcts in the corona radiata. We used the enriched dataset comprised of both image-based and alphanumeric databases to show that diffusion MR lesions overlapped in a more posterolateral brain location for patients with high NIH Stroke Scale scores (≥4) than for patients with low scores (≤3). In April 2009, we launched the first prospective image-based acute (≤1 week) stroke registry at our institution. The registered data include high signal intensity ischemic lesions on diffusion, T_2-weighted, or fluid attenuation inversion re-

This paper was presented in part at the 7th World Stroke Congress, Seoul, 2010.

KARGER

Fax +41 61 306 12 34
E-Mail karger@karger.ch
www.karger.com

1015–9770/11/0326–0567$38.00/0

Accessible online at:
www.karger.com/ced

Dong-Eog Kim, MD, PhD
814 Siksa-dong, Ilsan-ku
Goyang (Republic of Korea)
Tel. +82 31 961 7200
E-Mail kdongeog@duih.org

covery MRIs, and low signal intensity hemorrhagic lesions on gradient-echo MRIs. An interim analysis at 6 months showed that the time requirement for the lesion registration (183 consecutive patients, 3,226 MR slices with visible stroke-related lesions) was acceptable at about 1 h of labor per patient by a trained assistant with physician oversight. ***Conclusions:*** We have developed a novel image-based stroke registry, with database functions that allow the formulation and testing of intuitive, image-based hypotheses in a manner not easily achievable with conventional alphanumeric stroke registries.

Introduction

Conventional stroke registries contain alphanumeric text-based information about the clinical status and imaging findings of stroke patients. As was recently demonstrated by the Reduction of Atherothrombosis for Continued Health (REACH) registry [1], such registries play important roles in clinical practice and research by providing real-world statistical data of stroke-related queries [1–7].

However, the growth of imaging, particularly magnetic resonance imaging (MRI), has exposed a gap in our stroke registry design: MRI data are captured in a very abbreviated and filtered form, denying us the opportunity of easily subjecting the imaging data to future quantitative analysis [8–10]. Many stroke management decisions today are guided by imaging [11–13], leaving us with a growing disproportionality between the way stroke medicine is practiced and the data we capture in our registries. There is a need for a new kind of stroke registry to capture both clinical and imaging data.

To meet this need, we designed a next-generation stroke registry containing quantifiable brain MRI data and a software package to support this, and performed experiments to assess the feasibility and utility of the system. The software allows semiautomatic segmentation and transfer of lesions from the patient's clinical MRI onto a standard brain template set. Our system was designed to accept the clinical images used by physicians in hospitals to care for stroke patients as input, because we wanted to remain true to the actual day-to-day practice of a clinical stroke service. In this paper we show the software design and first implementation of our image-based stroke registry, data to show the technical performance of the software and early studies of clinical utility.

Methods

This study qualified for exemption from informed consent, and was approved by the institutional review board of Dongguk University Ilsan Hospital (DUIH), one of four community-based academic hospitals in a suburban city (Goyang) in the Seoul metropolitan area.

Conventional Alphanumeric and New Image-Based Stroke Registries

In January 2007, our institution joined a web-based nationwide acute stroke database project, the Korean Stroke Registry [5], which uses traditional alphanumeric data capture. As a new type of stroke database, the 'DUIH_Stroke-Registry-with-Images (DUIH_SRegI)' was designed to capture quantitative MRI data in a patient-independent visual format, interlinked with the alphanumeric data of the conventional stroke registry.

Development of a Software Package to Support an Image-Based Registry

All brain MRIs were acquired using a clinical 1.5-tesla MR machine (MAGNETOM-Avanto, Siemens, Erlangen, Germany). Source MRI data were converted into a patient-independent quantitative visual format by means of a custom-written software package: imaging software for quantitative neurovascular lesion assessment (Image_QNA). The essential functionality of the software is to transfer stroke-related lesions from raw MR images to a brain template, and to store and manipulate this visual information. The software was developed in Visual C++6.0 and open libraries, CxImage and GDI+. It was designed to take a balanced position between the convenience of currently available automatic registration software packages and the flexibility of manual registration, allowing us to deal with – less laboriously – any kind of MRI datasets regardless of acquisition protocols or specific equipment. Quantitative image analysis tools are provided to deal with various stroke-related queries; for example, color-coded composite maps can be generated, indicating the amount of spatial lesion overlap for user-specified patient groups.

Feasibility and Reliability of Image_QNA-Based Lesion Registration

From the 16,771 acute (≤1 week) stroke patients who had been prospectively registered at the Korean Stroke Registry (KSR) from January 2007 to December 2008, we admitted 474 to our hospital. We studied 47 consecutive patients (age 65.6 ± 13.5 years; 27 men and 20 women) with first-ever lacunar infarctions, of small vessel disease etiology on the TOAST (Trial of Org 10172 in Acute Stroke Treatment) classification [14], in the corona radiata on diffusion MRIs.

For a feasibility study of the software capabilities, a research assistant segmented and registered diffusion MR lesions of the patients onto a brain template set. A patient's fluid attenuation inversion recovery (FLAIR) MR images (four 5-mm-thick slices covering the corona radiata and internal capsule) were used as the brain template set. The template had a prespecified coordinate system for the brain and surrounding space, with the left lowermost coordinate: 0, 0 and right uppermost: 239, 249. The approximate center of the brain was located at the coordinate: 122, 122. Right hemisphere lesions were flipped horizontally to be located at the corresponding mirror position in the left hemisphere. An

experienced neurologist independently performed the same registration procedure twice, initially and after a 3-month interval, to validate interuser and intrauser reliability.

Next, we tested the variability of the lesion registration procedure between software packages. In 18 patients who were randomly selected from the above 47 patients, thin-section 3-dimensional T1-weighted MRIs were additionally obtained during routine clinical MR acquisitions. The results from the semiautomatic lesion registration using Image_QNA were compared with automatic lesion registration using SPM5 (Statistical Parametric Mapping version 5, http://www.fil.ion.ucl.ac.uk). In this study, the ch2better brain template that fits best to the Montreal Neurological Institute space (http://www.sph.sc.edu/comd/rorden/mricron/) was used. SPM5 software was used for spatial preprocessing and voxel-wise statistical analysis. Each 3-dimensional T_1-weighted MR image was spatially normalized onto the ch2better brain template. Both the affine transformation matrix and nonlinear local deformation field were obtained during the spatial normalization. Diffusion MRIs were then coregistered with the 3-dimensional T_1-weighted images in native space using a mutual information maximization algorithm and transformed into the standard space using the affine transformation matrix obtained during the spatial normalization of the 3-dimensional T_1-weighted image. The results of coregistration were checked using an image fusion program [15]. After a consensus meeting, two researchers, who were blinded to the software allocation, independently classified the quality of the registration in terms of lesion location, size and shape as 3 arbitrary categories: no, minor or major correction required.

Proof-of-Principle Experiments to Assess the Utility of an Image-Based Stroke Registry

In order to estimate the potential utility of an image-based stroke database, we used the registration data for these 47 patients for proof-of-principle experiments to test if the system could find factors associated with a higher National Institutes of Health Stroke Scale (NIHSS) score at admission. Based on published literature [16–19], we set up an a priori hypothesis: when lacunar stroke patients are divided into 2 groups based on a higher or lower admission NIHSS score, the locations of the composite lesions and/or infarct sizes would be different. We also tested if the 2 groups had any differences with regards to alphanumeric data, including demographic variables and risk factor variables. Moreover, we investigated if the system could distinguish the location of the corticobulbar tract from the location of the corti-cospinal tract by comparing the stroke lesions that caused dys-arthria without limb paresis (dysarthria-without-limb-paresis group, n = 10) and those lesions that caused limb paresis without dysarthria (limb-paresis-without-dysarthria group, n = 9).

Real-World Prospective Application of Image_QNA to Build the DUIH_SRegI Image-Based Stroke Database

As of April 2009, all consecutive patients admitted with acute (≤1 week) MRI-confirmed ischemic stroke had their MR lesions prospectively segmented and registered on the ch2better brain template. The registered data included high-signal-intensity ischemic lesions on diffusion, T_2-weighted, or FLAIR MRIs, and low-signal-intensity hemorrhagic lesions on gradient-echo MRIs. A trained research assistant performed the segmentation and registration under supervision of an experienced neurologist who could correct the data as needed. The time required for the registration of stroke-related MR lesions was measured. Detailed information about the alphanumeric variables of the new image-based stroke registry is available in the online supplementary material (www.karger.com/doi/10.1159/000331934).

Statistical Analysis

The Student t test was used for the comparison between groups of continuous variables and the χ^2 test was used to compare proportions. Bland-Altman plots were used to examine the level of agreement between registration outputs. An interrater reliability analysis using the kappa statistic was performed to determine consistency among raters. A statistical software package (SPSS 18.0, Chicago, Ill., USA) was used to conduct the analyses. A value of $p < 0.05$ was considered statistically significant.

Results

Software Package Operation

As presented in the figure 1 and movie 1, the Image_QNA enables users to segment stroke-related MR lesions semiautomatically and to register them on a standard brain template set. At first, MR source images are normalized to give the background a gray-scale pixel intensity of 0. Images are then rotated so that the interhemispheric fissure is vertical. After this, users can manually draw regions of interest (ROIs) containing stroke-related lesions to be segmented, and then click on any pixel of the lesions, followed by rolling the wheel of the computer mouse up or down in order to gradually exclude or include additional pixels of a similar signal intensity range. This lesion growing/shrinking method allows prompt and precise segmentation of multiple scattered lesions. Selected lesions are then aligned and registered onto the brain template. The segmented lesions are mapped automatically to the brain template using a mesh-warping algorithm and linear interpolation, laying two mesh grids over the source and template images. Finally, users can readjust the 2-dimensional orientation, shape and size of each registered lesion. When the resulting image dataset is saved to a database, the Image_QNA automatically extracts alphanumeric information from the source DICOM (digital imaging and communications in medicine) files: hospital ID, name, age, sex and type of image sequence. These data are saved together with the segmentation/registration data; they serve as a cross-reference linker between the alphanumeric dataset and the image dataset of the new stroke registry. This allows prompt loading of specific image files to match complex queries, including the text and numeric variables. Patients could

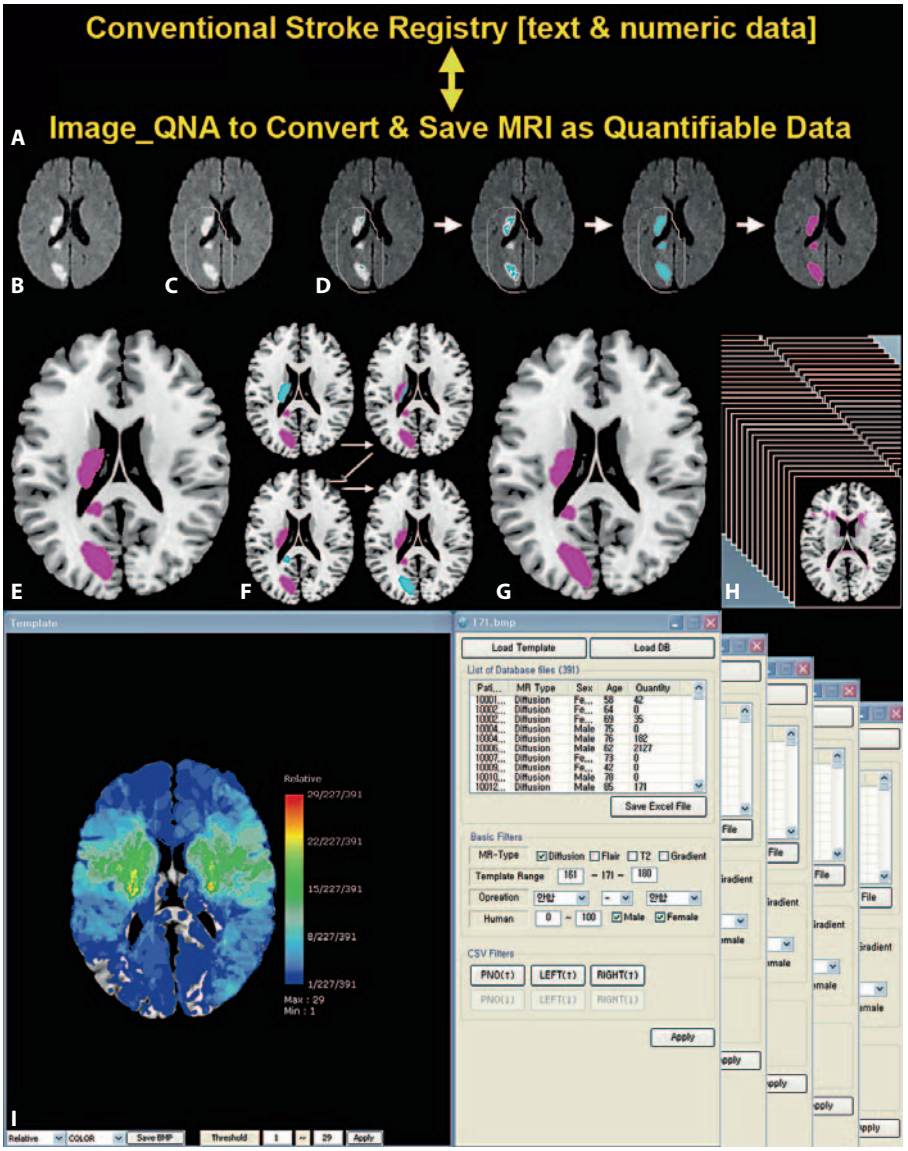

Fig. 1. Overview of the Image_QNA software package. **A** The purpose of the software is to segment and register MR lesions onto a brain template, allowing the linkage of quantitative MRI data to conventional stroke registries containing alphanumeric data fields. **B** A representative patient's diffusion MRI is loaded. **C** A user draws the ROI and clicks on any pixel inside the ROI. **D** The lesion thus selected can then be adjusted by the exclusion or inclusion of additional pixels of similar signal intensity range by rolling the wheel of the computer mouse up or down. **E–G** The selected lesion is then automatically transferred to a standard brain template, at which point the user can make fine adjustment to the location and size of the lesion using various tool buttons before saving the final data. **H**, **I** Once these registration procedures have been performed for each image slice needed, quantitative imaging analysis tools can be used on sets of MRI data of patient groups fulfilling user-specified research criteria.

be visually grouped together by generating lesion accumulation maps, in which added images are used to display the visual information of many patients on a single image set. Extensive analysis tools are available for image analysis operations on the accumulation maps, such as slice-by-slice adding, subtraction, intersection, or complementation of the selected images.

Performance of Lesion-to-Template Registration

Image_QNA-based registration of MR lesions showed low interuser and intrauser variability (fig. 2). Bland-Altman plots of the centroid coordinates (centers of the infarct lesions) or the infarct sizes, as measured by automatically calculated pixel counts, showed a high level of agreement between the registration outputs by the neurologist and those by the research assistant. Accordingly, lesion accumulation maps produced from separate registrations almost overlapped. As expected, intrauser agreement was better than interuser agreement.

Image_QNA-based semiautomatic MR lesion registration was superior to SPM5-based automatic registration in terms of lesion location, size and shape (table 1; fig. 3). Two independent blinded reviewers judged that 23–26 slices out of 29 in the Image_QNA group did not require any corrections. Three to 6 slices were categorized as requiring minor corrections. In contrast, in the

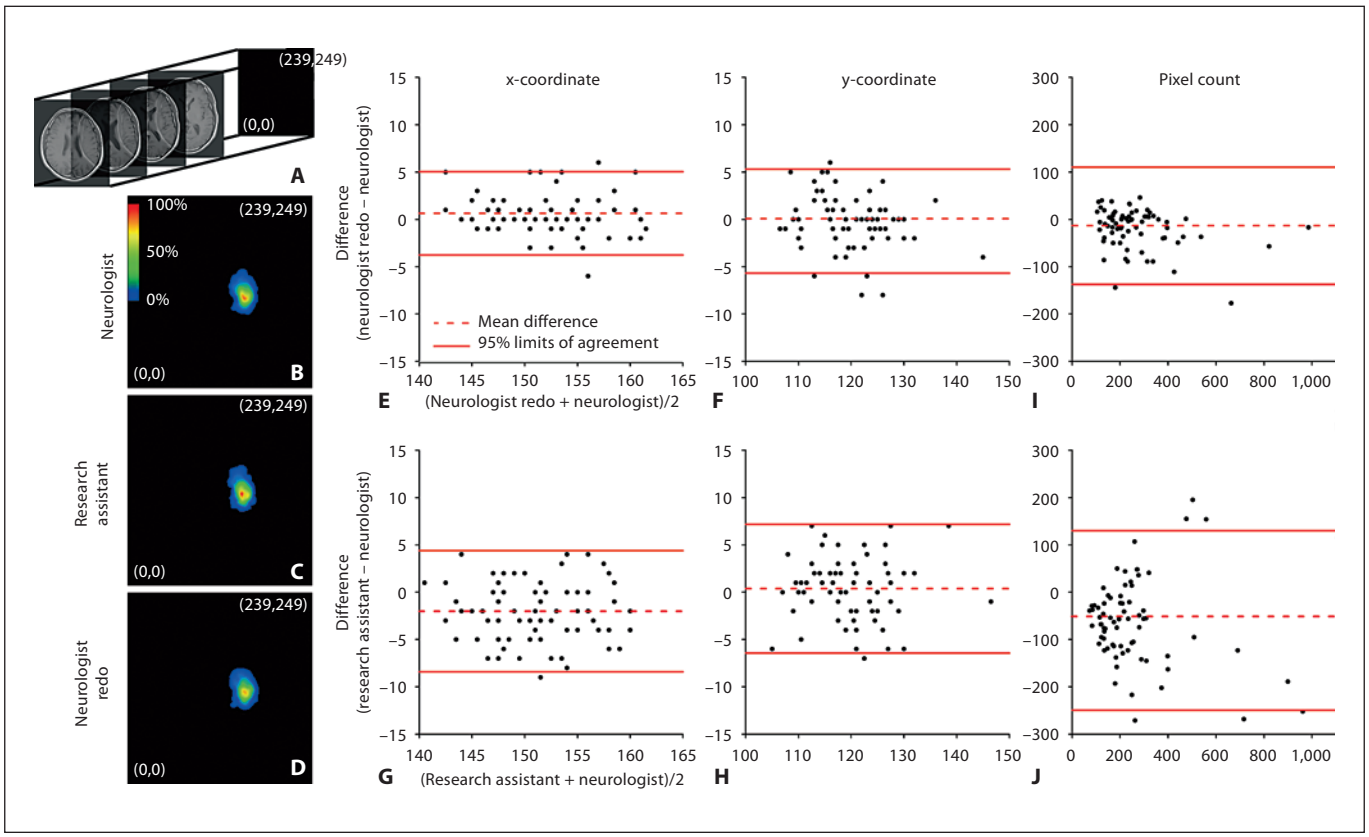

Fig. 2. Interuser and intrauser reliability of the Image_QNA software. Forty-seven lacunar infarcts were segmented and registered onto a brain template set by a neurologist (initially and 3 months later) and a research assistant (only initially). **A** Four slices in the brain template set were adequate to show these lesions; having been mapped to the template, all these lesions shared a common coordinate system. **B–D** The color-coded composite lesion maps produced from the registration data by the neurologist (1st registration) (**B**), a research assistant (**C**) and the neurologist (2nd registration at 3 months) (**D**) look visually similar indicating correspondence between them. **E–H** Bland-Altman plots of the centroid coordinates (centers of the infarct lesions) measure the agreement quantitatively, with a high level of agreement observed between each registration. **I**, **J** The extent of lesion size, expressed as pixel counts, also shows a high level of agreement between the registration outputs. The color scale denotes accumulation percentages.

SPM5 group 19–27 slices were judged to be requiring minor (n = 16–26) or major corrections (n = 0–5). Overall interrater reliability for the raters was found to be $\kappa = 0.62$ ($p = 0.00$).

Proof-of-Principle Experiments: Clinical Utility of an Image-Based Stroke Registry

The 47 lacunar infarct patients were divided into 2 groups based on the median admission NIHSS score (=3). The high NIHSS (≥4) group and low NIHSS (≤3) group did not show any statistical difference in terms of alphanumeric data (table 2).

However, when we produced lesion accumulation maps of each group using Image_QNA and the quantitatively registered MRI data, we did find a difference. The area of maximal lesion overlap was located more posterolaterally in the high NIHSS group than in the low NIHSS group (fig. 4A–D). This was corroborated by comparing the coordinates of the centers of the lesions, which was done after calculating the means of (x, y) coordinates provided by the software, of every individual patient, from all the template slices containing a lesion. The means of x-coordinates were higher, and hence more laterally located, in the high NIHSS group (151.8 ± 3.4) than in the low NIHSS group (149.0 ± 3.7, $p = 0.01$). The means of y-coordinates were lower, and hence more posteriorly located, in the high NIHSS group (116.9 ± 4.9) than in the low NIHSS group (121.9 ± 8.5, $p = 0.02$). In addition, the frequency of capsular involvement by downward extension of the corona radiata infarction was higher in the

high NIHSS group (71.4%) than in the low NIHSS group (42.3%, p = 0.049). However, the volumes of the lacunae, as measured by automatically calculated pixel counts, were not significantly different between the groups (601.0 ± 478.0 and 488.4 ± 437.9, respectively; p = 0.40).

In the lesion accumulation maps for the dysarthria-without-limb-paresis group (n = 10) and limb-paresis-without-dysarthria group (n = 7), the hot spots in all of the 4 template slices were located more anteriorly in the former than in the latter (fig. 4E–H). This was also corroborated by comparing the coordinates of the centers of the lesions. The means of y-coordinates were higher, hence more anteriorly located, in the dysarthria-without-limb-paresis group (128.1 ± 4.5) than in the limb-paresis-without-dysarthria group (116.0 ± 6.8; p = 0.00). The means of x-coordinates were slightly lower, hence more medially located, in the dysarthria-without-limb-paresis group (147.4 ± 4.6) than in the limb-paresis-without-dysarthria group (151.0 ± 3.2), which, however, showed only a marginal significance (p = 0.11). The sizes of cerebral infarctions were not statistically different between the dysarthria-without-limb-paresis group (708.8 ± 676.4) and the limb-paresis-without-dysarthria group (418.1 ± 244.5; p = 0.23).

Table 1. Accuracy of lesion registration: Image_QNA versus SPM5

Rater	Accuracy		Image_QNA	SPM5
1	Location	A	26	6
		B	3	22
		C	0	1
	Shape	A	26	2
		B	3	26
		C	0	1
	Size	A	26	3
		B	3	26
		C	0	0
2	Location	A	23	10
		B	6	16
		C	0	3
	Shape	A	23	4
		B	6	20
		C	0	5
	Size	A	24	4
		B	5	22
		C	0	3

A = No correction required; B = minor correction required; C = major correction required.

Table 2. Demographic, clinical and imaging variables of the patients for the proof-of-principle experiments

	Admission NIHSS		p value[a]
	low (0–3) (n = 26)	high (≥4) (n = 21)	
Median admission NIHSS	2	5	
Age, years	66.7 ± 12.4	64.3 ± 15.0	0.56
Sex, male	14 (53.8)	13 (61.9)	0.12
Hypertension	15 (57.7)	13 (61.9)	0.69
Diabetes mellitus	9 (34.6)	3 (14.3)	0.12
Smoking history	13 (50.0)	11 (52.4)	0.74
Hyperlipidemia	7 (26.9)	7 (33.3)	0.59
Statin medication	6 (23.1)	1 (4.8)	0.08
Total cholesterol, mmol/l	4.5 ± 0.7	4.7 ± 0.9	0.56
High-density lipoprotein cholesterol, mmol/l	1.1 ± 0.3	1.2 ± 0.3	0.16
Low-density lipoprotein cholesterol, mmol/l	2.6 ± 0.6	2.8 ± 0.8	0.46
Triglyceride, mmol/l	1.7 ± 1.0	1.5 ± 0.8	0.50
Admission systolic blood pressure, mm Hg	147.5 ± 18.9	157.4 ± 19.8	0.09
Admission diastolic blood pressure, mm Hg	82.9 ± 13.7	86.1 ± 8.8	0.36
Infarct extension to the capsular area	11 (42.3)	15 (71.4)	0.046
Infarct size, pixel counts	488.4 ± 437.9	601.0 ± 478.0	0.40
Infarct location, mean x-coordinate	149.0 ± 3.7	151.8 ± 3.4	0.01
Infarct location, mean y-coordinate	121.9 ± 8.5	116.9 ± 4.9	0.02

Values are presented as means ± standard deviations or as frequencies (percentages).
[a] Student's t test or χ^2 test.

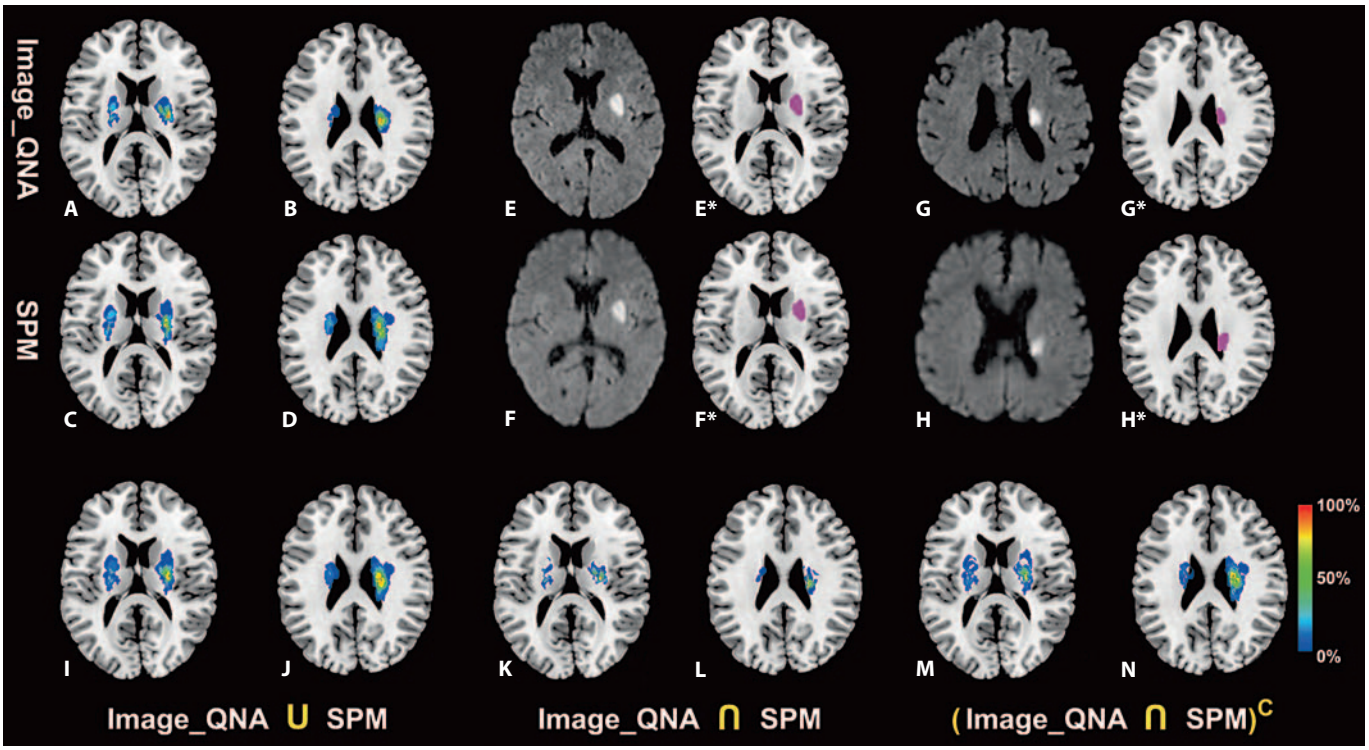

Fig. 3. Comparison between the color-coded lesion accumulation maps of diffusion MRIs produced using the Image_QNA software versus SPM5. **A–D** The Image_QNA-based and SPM-based lesion accumulation maps (n = 18 patients) look similar but do not match each other exactly (**A–C** and **B–D**). **E**, **F*** In the representative patient whose registration maps were of an acceptable accuracy regardless of the software used (**E**, **E*** and **F**, **F***), the SPM-mediated normalized-and-transformed diffusion MRI (**F**) had an infarct lesion with a size and location similar to the original image (**E**). **G**, **H*** However, in the representative patient whose registration maps did not correlate with each other depending on the software used (**G**, **G*** and **H**, **H***), the automatic normalization and transformation by the SPM turned out to have distorted the original diffusion MRI (**G**) into one with the infarct lesion displaced and deformed (**H**), which resulted in the inaccurate registration of the lesion on the template (**H***). **I–N** Consequently, the maps of the union between the Image_QNA-based and SPM-based registrations (**I**, **J**) do not correlate with those of the intersection operation (**K**, **L**) but with those of the complementation operation (**M**, **N**). The color scale denotes accumulation percentage.

The First Prospective Image-Based Acute Stroke Registry, DUIH_SRegI Database: Time Requirement for the Registration of Stroke-Related MR Lesions

During the 6-month period after the initiation of the DUIH_SRegI, 183 consecutive patients (age 68.3 ± 11.4, 100 men/83 women) admitted with acute ischemic stroke were registered. As summarized in table 3, the mean time per patient required for the segmentation and registration of every MR lesion (3,226 MR slices) was 60.4 ± 44.4 min: diffusion MRI (20.6 ± 27.7 min), T_2-weighted MRI (6.7 ± 11.2 min), FLAIR MRI (33.9 ± 26.9 min) and gradient-echo MRI (3.4 ± 7.0 min). A longer time was required for the MRIs of the patients with cardioembolic (97.9 ± 36.0 min) or large artery disease stroke (80.6 ± 43.5 min), compared with small vessel disease stroke (46.4 ± 39.6 min) or transient ischemic attack (16.7 ± 15.9 min).

Discussion

In this study, we introduce a new image-based stroke database, DUIH_SRegI, containing quantitative imaging data in addition to the alphanumeric data currently captured in conventional stroke registries. The combined imaging and alphanumeric dataset described is currently being used to prospectively collect data in a consecutive manner. This represents one of the most comprehensive existing stroke registry datasets of which we are aware. Having image- and text-based information interlinked will facilitate new depths of inquiry in stroke research.

The Image_QNA software package that we developed to generate and support the image-based stroke database enabled research assistants to segment stroke-related le-

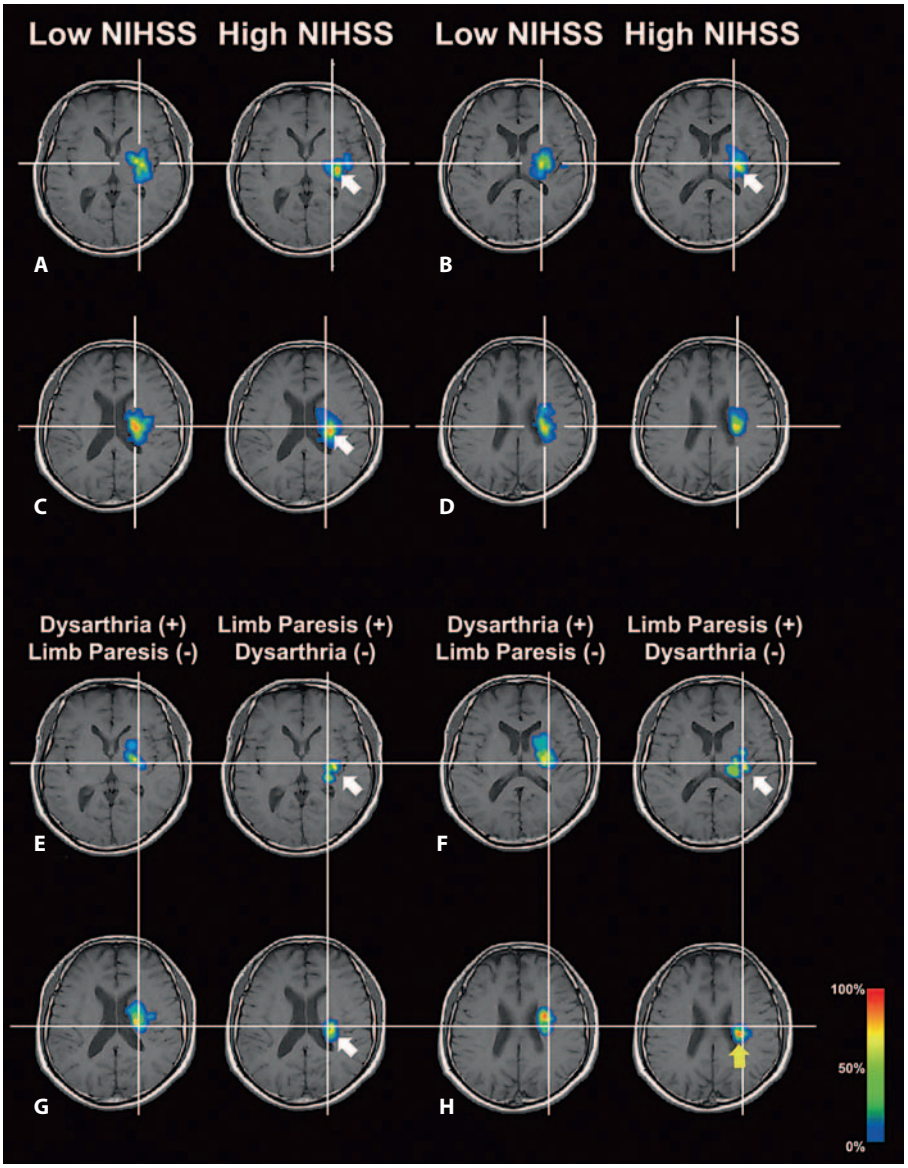

Fig. 4. Color-coded lesion accumulation maps of diffusion MRIs for patients with acute lacunar infarcts. **A–D** In 3 (**A–C**) of 4 brain template slices (**A–D**), the infarct area the most overlapped is located more posterolaterally in the high (≥4) NIHSS group than in the low (0–3) NIHSS group (arrows). **E–H** In all 4 templates, the infarct area overlapped the most is located more posterolaterally (white arrows) or posteriorly (yellow arrow) in the limb-paresis-without-dysarthria group than in the dysarthria-without-limb-paresis group. The color scale denotes the percentage of patients having a lesion at that pixel location.

Table 3. Average time requirement, min/patient (min/slice), for the registration of stroke-related MR lesions (183 patients, 3,226 MR slices) to the ch2better template to build the DUIH_SRegI

TOAST [1]	Diffusion MRI	T_2-weighted MRI	FLAIR MRI	GE MRI	Total
TIA (n = 11)	3 (1.5)[a]	1.8 ± 2.5 (1.7 ± 0.6)	16.3 ± 12.0 (2.7 ± 0.9)	–	20.5 ± 27.6 (2.3 ± 0.7)
LAD (n = 48)	36.8 ± 35.6 (2.8 ± 1.2)	5.9 ± 8.3 (3.0 ± 1.2)	36.9 ± 20.4 (4.1 ± 1.4)	3.2 ± 7.1 (2.8 ± 0.9)	80.6 ± 43.5 (3.2 ± 0.9)
SVD (n = 82)	7.8 ± 6.8 (2.3 ± 1.0)	5.3 ± 8.2 (2.9 ± 0.9)	31.8 ± 32.8 (4.1 ± 2.7)	3.4 ± 5.8 (3.1 ± 1.2)	46.4 ± 39.6 (3.3 ± 1.9)
CE (n = 12)	50.5 ± 38.1 (2.9 ± 1.1)	12.4 ± 14.4 (3.4 ± 1.2)	44.9 ± 25.7 (4.4 ± 1.9)	7.4 ± 14.0 (3.1 ± 1.4)	97.9 ± 36.0 (3.3 ± 0.9)
UD (n = 29)	26.3 ± 25.6 (2.5 ± 1.2)	12.5 ± 19.7 (4.9 ± 7.1)	35.4 ± 17.3 (4.1 ± 2.0)	3.2 ± 6.9 (3.4 ± 1.0)	73.3 ± 43.3 (3.4 ± 1.2)
Total (n = 183)	20.6 ± 27.7 (2.5 ± 1.1)	6.7 ± 11.2 (3.3 ± 3.4)	33.9 ± 26.9 (4.0 ± 2.2)	3.4 ± 7.0 (3.1 ± 1.1)	60.4 ± 44.4 (3.3 ± 1.5)

CE = Cardioembolism; FLAIR = fluid attenuation inversion recovery; GE = gradient-echo; LAD = large artery disease; SVD = small vessel disease; TIA = transient ischemic attack; UD = undetermined.

[a] One of the 11 TIA patients had visible lesions on the diffusion MRI (2 slices).

sions on diffusion, T_2-weighted, FLAIR and gradient-echo MRIs semiautomatically, and to register them on a standard brain template set. It was easily applicable to routine brain MR studies obtained in clinical practice, and while manual labor is required, the time requirement of about 1 h per patient was acceptable. Our stroke team has about 300 acute ischemic stroke patients admitted every year, corresponding to a workload of about 300 h per year. A similar amount of time is additionally required for administrative overheads such as the collection and management of image files and general administration. Our experience indicates that – with our workload – a well-trained half-time assistant could keep the imaging part of the image-based stroke database working.

We had an experienced neurologist carefully verify all the work of our research assistants, and found that major editing was infrequently required with regard to the size and location of registered MR lesions. When researchers independently segmented and registered diffusion MR lesions, the spatial correlation of the centers of the lesions was high, and the lesion maps from each registration almost overlapped. Intrauser correlation was better than interuser correlation. In our hands, the Image_QNA-based semiautomatic method produced more accurate results than the SPM-based automatic method, arguing strongly for the role of user input to supervise algorithms such as these.

To show the clinical usefulness of an image-based registry containing quantitative MR data, we tested, in a retrospective analysis, the hypothesis that the locations of the composite lesions and/or infarct sizes would correlate to stroke severity at admission. We studied 47 consecutive patients with a first-ever acute lacunar infarction in the corona radiata, and divided them into 2 groups: high NIHSS and low NIHSS. Besides the NIHSS scores, the alphanumeric data captured on these patient groups (demographic and risk factors) were similar, with no distinction possible between the groups. However, the composite quantitative MR data maps generated by the Image_QNA software revealed a significant intergroup difference apparent only on imaging data. Infarcts were located more posterolaterally in the high NIHSS group than in the low NIHSS group. This follows from the anatomy of the corticospinal tract passing posterolaterally to the corticobulbar tract, which could be reconfirmed by using the Image_QNA software: there were clear differences, with dysarthria-causing lesions being more anteriorly located than limb-weakness-causing lesions that were more posteriorly located. This points out a scoring anomaly in the NIHSS system: scores for the dysarthria have a range of 1–3 points, whereas those for the limb weakness have a wider range: 1–8 points. Moreover, hemiplegia scoring 8 points could be caused by a small unilateral stroke lesion, but dysarthria severe enough to score 3 points would usually require multiple, bilateral, or bigger stroke lesions. These imply that there is no one-to-one correlation between stroke severity and NIHSS, leaving stroke researchers with a possible discordance that cannot be resolved without reference to imaging findings. Our results support previous studies [16, 17, 19] that highlighted the importance of lesion location affecting the neurological deficit of stroke patients. Again, this illustrates the usefulness of an image-based stroke database supplementing conventional alphanumeric databases in stroke research.

Our image-based database system has limitations. It stands to reason that patients who cannot undergo MRI for whatever reason are excluded from the visual database, although their alphanumeric data will still be registered. Motion artifacts, tissue distortion, or metallic artifact will render some images uninterpretable; this will preclude high-quality registration and lead to such patients being excluded from final analyses. These factors might bias the database in favor of patients who are clinically stable or have less severe strokes. In addition, retrospective hospital-based data mining may limit the value of this type of system in the absence of prospective studies with a specific a priori hypothesis. We recently began to implement our approach prospectively on a national level, with strict quality control (using a 5-point grading of registration quality) to help avoid potential biases such as the ones described above (online suppl. tables 1S, 2S, video).

In summary, we have developed a new image-based acute stroke database with a custom-built software package to support it. This allows visual image-based data to be interlinked with traditional alphanumeric data in a comprehensive stroke registry. The augmented registry design will allow the formulation and testing of intuitive, text-/image-based hypotheses in a manner not easily achievable with conventional alphanumeric stroke registries.

Acknowledgments

The authors would like to thank Dr. Il-Young Jung and stroke research nurses Eun-Kyoung Hwang, Dong-Hee Kang and Jeong-Eun Park, who helped with data collection. This study was supported by grants (A070001 and A08020 to Dr. D.-E. Kim) of the Korea Healthcare Technology R&D Project, Ministry of Health and Welfare, Republic of Korea.

References

1 Bhatt DL, Steg PG, Ohman EM, Hirsch AT, Ikeda Y, Mas JL, Goto S, Liau CS, Richard AJ, Rother J, Wilson PW: International prevalence, recognition, and treatment of cardiovascular risk factors in outpatients with atherothrombosis. JAMA 2006;295:180–189.

2 Caplan LR, Wityk RJ, Glass TA, Tapia J, Pazdera L, Chang HM, Teal P, Dashe JF, Chaves CJ, Breen JC, Vemmos K, Amarenco P, Tettenborn B, Leary M, Estol C, Dewitt LD, Pessin MS: New England Medical Center Posterior Circulation Registry. Ann Neurol 2004;56:389–398.

3 Carrera E, Maeder-Ingvar M, Rossetti AO, Devuyst G, Bogousslavsky J: Trends in risk factors, patterns and causes in hospitalized strokes over 25 years: the Lausanne stroke registry. Cerebrovasc Dis 2007;24:97–103.

4 Kumral E, Ozkaya B, Sagduyu A, Sirin H, Vardarli E, Pehlivan M: The Ege Stroke Registry: a hospital-based study in the Aegean region, Izmir, Turkey. Analysis of 2,000 stroke patients. Cerebrovasc Dis 1998;8:278–288.

5 Lee BC, Roh JK: International experience in stroke registries: Korean stroke registry. Am J Prev Med 2006;31:S243–S245.

6 Michel P, Odier C, Rutgers M, Reichhart M, Maeder P, Meuli R, Wintermark M, Maghraoui A, Faouzi M, Croquelois A, Ntaios G: The Acute Stroke Registry and analysis of Lausanne (ASTRAL): design and baseline analysis of an ischemic stroke registry including acute multimodal imaging. Stroke 2010;41:2491–2498.

7 Moulin T, Tatu L, Crepin-Leblond T, Chavot D, Berges S, Rumbach T: The Besançon Stroke Registry: an acute stroke registry of 2,500 consecutive patients. Eur Neurol 1997;38:10–20.

8 Enzinger C, Ropele S, Gattringer T, Langkammer C, Schmidt R, Fazekas F: High-grade internal carotid artery stenosis and chronic brain damage: a volumetric magnetic resonance imaging study. Cerebrovasc Dis 2010;30:540–546.

9 Galinovic I, Brunecker P, Ostwaldt AC, Soemmer C, Hotter B, Fiebach JB: Fully automated postprocessing carries a risk of substantial overestimation of perfusion deficits in acute stroke magnetic resonance imaging. Cerebrovasc Dis 2011;31:408–413.

10 Tiehuis AM, Vincken KL, Mali WP, Kappelle LJ, Anbeek P, Algra A, Biessels GJ: Automated and visual scoring methods of cerebral white matter hyperintensities: relation with age and cognitive function. Cerebrovasc Dis 2008;25:59–66.

11 Adams H, Adams R, Del Zoppo G, Goldstein LB: Guidelines for the early management of patients with ischemic stroke: 2005 guidelines update a scientific statement from the stroke council of the American Heart Association/American Stroke Association. Stroke 2005;36:916–923.

12 Adams RJ, Albers G, Alberts MJ, Benavente O, Furie K, Goldstein LB, Gorelick P, Halperin J, Harbaugh R, Johnston SC, Katzan I, Kelly-Hayes M, Kenton EJ, Marks M, Sacco RL, Schwamm LH: Update to the AHA/ASA recommendations for the prevention of stroke in patients with stroke and transient ischemic attack. Stroke 2008;39:1647–1652.

13 Latchaw RE, Alberts MJ, Lev MH, Connors JJ, Harbaugh RE, Higashida RT, Hobson R, Kidwell CS, Koroshetz WJ, Mathews V, Villablanca P, Warach S, Walters B: Recommendations for imaging of acute ischemic stroke: a scientific statement from the American Heart Association. Stroke 2009;40:3646–3678.

14 Adams HP, Woolson RF, Clarke WR, Davis PH, Bendixen BH, Love BB, Wasek PA, Grimsman KJ: Design of the Trial of Org 10172 in Acute Stroke Treatment (TOAST). Control Clin Trials 1997;18:358–377.

15 Lee JS, Park KS, Lee DS, Lee CW, Chung JK, Lee MC: Development and applications of a software for functional image registration (FIRE). Comput Methods Programs Biomed 2005;78:157–164.

16 Kim JS, Pope A: Somatotopically located motor fibers in corona radiata: evidence from subcortical small infarcts. Neurology 2005;64:1438–1440.

17 Menezes NM, Ay H, Wang Zhu M, Lopez CJ, Singhal AB, Karonen JO, Aronen HJ, Liu Y, Nuutinen J, Koroshetz WJ, Sorensen AG: The real estate factor: quantifying the impact of infarct location on stroke severity. Stroke 2007;38:194–197.

18 Saver JL, Johnston KC, Homer D, Wityk R, Koroshetz W, Truskowski LL, Haley EC: Infarct volume as a surrogate or auxiliary outcome measure in ischemic stroke clinical trials. Stroke 1999;30:293–298.

19 Song YM: Somatotopic organization of motor fibers in the corona radiata in monoparetic patients with small subcortical infarct. Stroke 2007;38:2353–2355.